Nanostructure instability induced by anisotropic epitaxial stresses

Jérôme Colin* and Jean Grilhé
PHYMAT-CNRS UMR 6630, Université de Poitiers, BP 30179, 86962 Futuroscope Cedex, France

Pierre Müller
CINaM-CNRS, UPR 3118, Université d'Aix-Marseille, Campus de Luminy, Case 913, 13288 Marseille Cedex, France
(Received 26 May 2009; published 5 November 2009)

The morphological evolution of an initially straight stripe assimilated to a straight line of infinite length lying on a semi-infinite substrate has been investigated in the linear regime when the mass transport mechanism is the diffusion of adatoms along stripe edges and when the heteroepitaxy between the line and the substrate is taken to be anisotropic. It is found that contrary to the isotropic case where serpentine-like morphology is favored, antiphase fluctuations grows faster than in-phase ones for selected values of epitaxial stress components such that a pinched shape preferentially emerges.

DOI: 10.1103/PhysRevE.80.052601 PACS number(s): 81.15.Aa, 68.35.Ct, 68.35.Fx, 81.15.Hi

Understanding morphological instabilities of surfaces submitted to an external field is a key point for developing nanostructured materials. Vicinal surfaces are known to exhibit morphological instabilities induced by many different driving forces. It is for instance the case during step flow growth where according to the relative properties of diffusion of adatoms on the terraces and their incorporation in the steps, in-phase step meandering or step-bunching can be predicted and observed (see [1,2] and review [3]). Likewise, an external electric field may drive kinetic instabilities [4–9]. The final surface morphology (bunching, meandering [3], or even faceting [10]) depends upon the current direction, and the sample temperature as illustrated for silicon [11] where for a given current direction, bunching supersedes meandering above a critical temperature. Another driving force for instabilities is elasticity (for reviews see [3,12]). Indeed, externally applied stresses or epitaxial stresses modify the elastic interactions between steps which thus engender different surface configurations. In particular, the effect of stress on step meandering has been investigated for homoepitaxy [13,14]. In the case of isotropic heteroepitaxy, it has been found that elasticity favors the development of out-of-phase fluctuations for the step profiles with a phase shift of π [15].

In this work, one focuses on stress-driven instabilities of a straight line epitaxially stressed on a semi-infinite substrate which can model monaoatomic stripes but also higher structures (but still at the nanoscale). The formation of such stripes has been observed in many experimental situations. The formation of arrays of parallel Fe stripes have been for example observed on Cu(111) substrates [16–18] and has been modeled by means of molecular dynamic simulations [19]. Likewise, monoatomic Co wires have been realized on vicinal Pt(997) surfaces [20,21]. The formation of regularly spaced stripes have been also observed on Cu{110}$-(2\times1)$O surfaces from the rearrangement of anisotropic islands [22] as well as nanowires on the surface of thin carbon films which have been produced using electron-beam-induced deposition techniques [23]. The effects of different stresses on the shape of nanostructures such as stripes, islands and dots have been investigated in the framework of continuum elasticity theory [13,24–27]. When surfaces reconstruct with broken orientational symmetry for example, it has been found that the formation of striped domains may be favorable depending on intrinsic stress, the periodicity of these domains when they exist being then determined [28]. The development of thin films on substrates with particular dielectric or magnetic properties has also shown that anisotropic heteroepitaxial stresses may arise resulting from the difference between the lattice networks of the films and the substrates, from crystallographic disorientations at the interfaces or due to defects such as misfit dislocations leading to nonhomogeneous strain relief along the different crystallographic directions [29,30]. In the context of nanoelectronics, recent papers have been devoted to the fabrication at higher scale of strained lines (width: a few tens of nm, height: roughly 10 nm, and length: 1 mm), the control of their stability being of great importance in transistor technology [31,32].

For the sake of simplicity, a single epitaxially stressed stripe of infinite length is considered in this Brief Report when the stripe evolves at constant volume by edge diffusion. It is believed that the main results obtained in this work concerning the effects of anisotropic stress on the nanostructure morphology would be generalized to the more complex configuration where several stripes are growing (or shrinking) in presence of diffusion currents on the surface like during step flow growth (or sublimation) regime. In the following, the effects of stress resulting from an anisotropic heteroepitaxy between the stripe and the substrate has been modeled within the framework of force monopole approximation and linear elasticity. The possibility of formation of pinched or serpentine-like shapes by edge diffusion under the action of the resulting biaxial stresses is discussed.

A line of width l, height h, and infinite length is considered on a semi-infinite substrate in the general case where the heteroepitaxy between the stripe and the substrate is anisotropic (see Fig. 1 for axes). To model the elastic effects in the stripe and the substrate resulting from the anisotropic epitaxy along the (Ox) and (Oy) directions, the following distribu-

*jerome.colin@univ-poitiers.fr

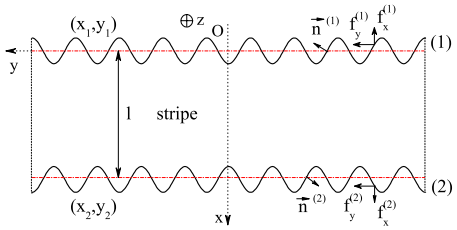

FIG. 1. (Color online) Top view of a morphologically unstable stripe of width l epitaxially stressed on a substrate. Along the ith edge (with $i=1,2$), two distributions of force monopoles $f_x^{(i)}$ and $f_y^{(i)}$ are considered to model the effects onto the development of edge fluctuations of the two constant stress components σ_{xx}^0 and σ_{yy}^0 resulting from the anisotropic epitaxy.

tion of force monopoles along the kth stripe edge is considered [13,15,24–26,28,33]

$$f_x^{(k)}(\rho) = -h\sigma_{xx}^0 \delta(\rho-\rho_k) n_x^{(k)}, \tag{1}$$

$$f_y^{(k)}(\rho) = -h\sigma_{yy}^0 \delta(\rho-\rho_k) n_y^{(k)}, \tag{2}$$

with $\rho=(x,y)$, $\rho_k=(x_k,y_k)$ is the position of the kth edge, δ is Dirac's function, $\mathbf{n}^{(k)}$ is the outward normal to edge k, σ_{xx}^0 and σ_{yy}^0 are the two constant epitaxial stress components, and $k=1,2$. Notice that the surface stress contribution has been neglected in Eqs. (1) and (2). This point will be discussed later. A standard linear stability analysis of the stripe under epitaxial stresses has been conducted. To do so, both edge profiles are perturbed as follows $x_1=\zeta_1(y_1)=\epsilon\cos(qy_1)$ and $x_2=l+\zeta_2(y_2)=l+\epsilon\cos(qy_2+\varphi)$ with ϵ, q, and φ the amplitude, wave number, and phase shift of the fluctuations, respectively. The elastic energy due to the interactions between both edges defined by [15,24–26,28,33]

$$\mathcal{F}_{el}^{int} = -\int_S \int_S d^2\rho d^2\rho' f_i^{(1)}(\rho) f_j^{(2)}(\rho') \chi_{ij}(\rho-\rho'), \tag{3}$$

has been then developed to the second order in perturbation amplitude ϵ, with S the substrate surface and $\chi_{ij}(\rho)=\chi_{ij}(\rho,z=0)$ the surface elastic Green's function determined for a semi-infinite solid in the framework of linear and isotropic elasticity [33]. The self-energy term $\mathcal{F}_{el}^{self,i}$ of each edge i has also to be considered. It must be independent of the phase shift between the two perturbations and has been defined to the second order in ϵ following the procedure used to evaluate the elastic self-energy of a dipole of dislocations [34]. In Eq. (3), taking $l=a$ with a a cut-off distance of the order of the interatomic distance and using two in-phase perturbations $\zeta_i(y_i)$ for step i, $\mathcal{F}_{el}^{self,i}$ has been defined as $\mathcal{F}_{el}^{self,i}=-1/2\mathcal{F}_{el}^{int}$. It yields that the total elastic energy $\mathcal{F}_{el}=\mathcal{F}_{el}^{int}+\mathcal{F}_{el}^{self,1}+\mathcal{F}_{el}^{self,2}$ cancels when two in-phase perturbed edges are brought closer until the cut-off distance a. The elastic contribution $\mu_{el}^{(2)}$ to the chemical potential of edge 2,

$$\mu_{el}^{(2)} = \Omega\left(\frac{\delta F_{el}^{int}}{\delta\zeta_2(y_2)} + \frac{\delta F_{el}^{self,2}}{\delta\zeta_2(y_2)}\right), \tag{4}$$

has been then determined to the first order in ϵ with Ω the atomic area [15]. The heavy but straightforward derivation of $\mu_{el}^{(2)}$ is not detailed in the Brief Report. It yields

$$\mu_{el}^{(2)} = \frac{2(1+\nu)(h\sigma_{xx}^0)^2\Omega}{\pi E}\left\{\psi(l,\varphi) - \frac{1}{2}\psi(a,0)\right\}\zeta_2(y_2), \tag{5}$$

with

$$\psi(x,\phi) = \frac{1}{x^2}\int_{-\infty}^{+\infty}\left[\frac{15(1-\sigma)\nu}{(1+z^2)^{7/2}} + \frac{3-18\nu+15\nu\sigma}{(1+z^2)^{5/2}} + \frac{3\nu-1-2\nu\sigma}{(1+z^2)^{3/2}}\right][1-\cos(\phi)\cos(qxz)]dz + \cos(\phi)\frac{q}{x}\int_{-\infty}^{+\infty}\left[\frac{(\sigma-\nu)\sigma z}{(1+z^2)^{3/2}} + \frac{3(1-\sigma)\sigma\nu z}{(1+z^2)^{5/2}}\right]\sin(qxz)dz, \tag{6}$$

where E is the Young modulus, ν the Poisson's ratio and $\sigma=\sigma_{yy}^0/\sigma_{xx}^0$ the ratio of stress components characterizing the anisotropy of the epitaxy. Using Eqs. (5) and (6), the elastic contribution to the chemical potential of edge 2 has been finally found to be

$$\mu_{el}^{(2)} = \frac{4(1+\nu)(h\sigma_{xx}^0)^2\Omega}{\pi E l^2}\left[\eta(\tilde{q},\varphi) - \frac{1}{2\tilde{a}^2}\eta(\tilde{a}\tilde{q},0)\right]\zeta_2(y_2), \tag{7}$$

with

$$\eta(x,\phi) = 1-\nu+x\{x(\sigma-1)(1+\sigma-2\nu)K_0(x) + \{-1+[1-x^2(\sigma-1)^2]\nu\}K_1(x)\}\cos(\phi), \tag{8}$$

$\tilde{q}=ql$, $\tilde{a}=a/l$, and K_0 and K_1 are the modified Bessel's functions of second kind of the zero and first order, respectively. An equivalent expression holds for $\mu_{el}^{(1)}$, the elastic contribution to the chemical potential of edge 1. The contribution to the chemical potential μ_2 of the edge line free energy is $\mu_{fr}^{(2)}=\gamma\Omega\kappa_2(y_2)$, with γ the edge stiffness and κ_2 the local curvature of edge 2 taken to be positive for a convex profile. To the first order in ϵ, it yields $\mu_{fr}^{(2)}=\gamma\Omega\tilde{q}^2\zeta_2(y_2)/l^2$. The chemical potential of edge 2 is then given by

$$\mu_2 = \mu_{fr}^{(2)} + \mu_{el}^{(2)}, = \frac{\Omega\gamma}{l^2}\left\{\tilde{q}^2 + \beta\left[\eta(\tilde{q},\varphi) - \frac{1}{2\tilde{a}^2}\eta(\tilde{a}\tilde{q},0)\right]\right\}\zeta_2(y_2), \tag{9}$$

with $\beta=4(1+\nu)(h\sigma_{xx}^0)^2/(\pi E\gamma)$. Assuming now that atoms diffuse along both edges, the normal velocity of edge 2 is [14]

$$v_{n_2} = a_L\left[\partial_{s_2} D_L \partial_{s_2}\left(\frac{\mu_2}{k_B T}\right)\right], \tag{10}$$

with a_L the lattice spacing, D_L the mobility of atoms taken to be constant along both edges of the stripe, s_2 the arclength along the edge 2, k_B the Boltzmann's constant and T the absolute temperature. Introducing the expression of μ_2 [see Eq. (9)] in Eq. (10), the evolution of the perturbation amplitude versus the dimensionless time $\tau=a_L D_L\Omega\gamma/(l^4 k_B T)t$ is

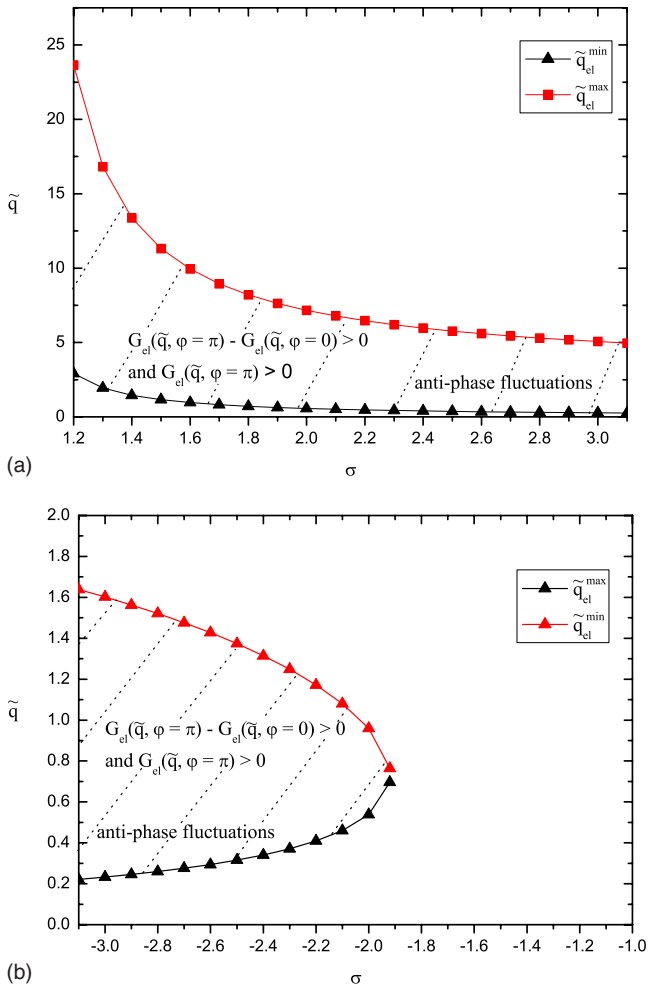

FIG. 2. (Color online) Positive values of $G_{el}(\tilde{q},\varphi=\pi) - G_{el}(\tilde{q},\varphi=0)$ in the $(\sigma,\tilde{q})$ plane. (a) Case of positive stress ratio $\sigma=\sigma_{yy}^0/\sigma_{xx}^0$. (b) Case of negative σ.

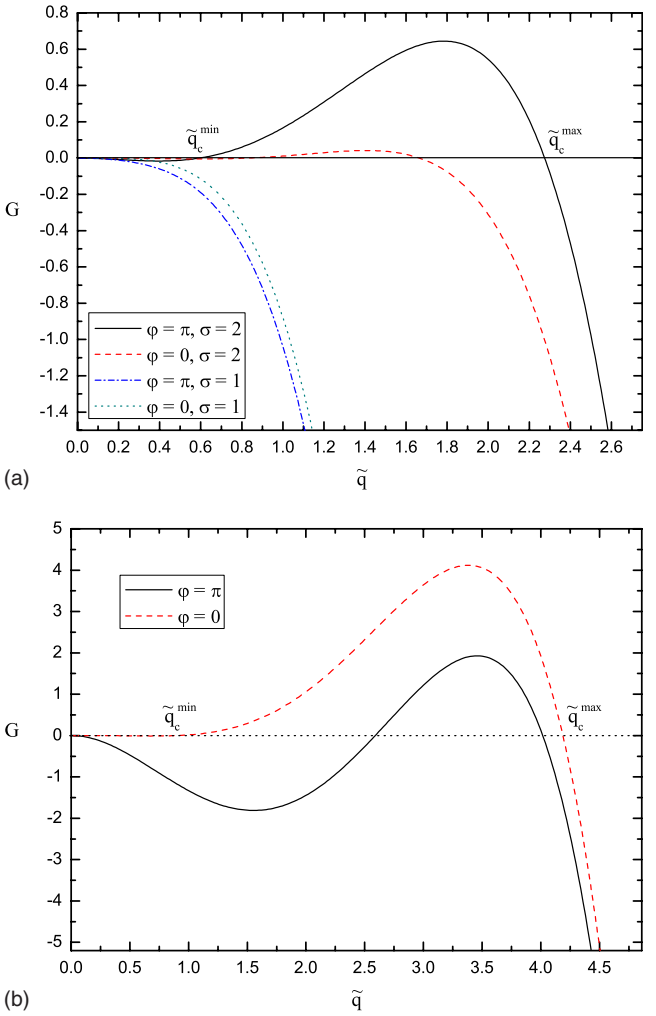

FIG. 3. (Color online) G as a function of $\tilde{q}$ for $\varphi=\pi$ and $\varphi=0$. (a) For $\beta=0.19$, case of isotropic epitaxy $\sigma=1$ and anisotropic epitaxy $\sigma=2$. (b) For $\beta=1.6$, case of isotropic epitaxy $\sigma=1$.

$$\frac{d\epsilon}{d\tau} = \epsilon G(\tilde{q},\varphi), \tag{11}$$

with G the growth rate of the perturbation,

$$G(\tilde{q},\varphi) = \tilde{q}^2\left\{-\tilde{q}^2 + \beta\left[\frac{1}{2\tilde{a}^2}\eta(\tilde{a}\tilde{q},0) - \eta(\tilde{q},\varphi)\right]\right\}. \tag{12}$$

The resolution of the surface diffusion equation along edge 1 leads to the same expression of the fluctuation growth rate as the one displayed in Eq. (12). Since the variation of the elastic contribution to the growth rate $G_{el}(\tilde{q},\varphi) = \tilde{q}^2[\eta(\tilde{a}\tilde{q},0)/(2\tilde{a}^2) - \eta(\tilde{q},\varphi)]$ versus φ has been found to be extremum for $\varphi=0$ and $\varphi=\pi$, only in-phase ($\varphi=0$) and antiphase ($\varphi=\pi$) fluctuations have been studied in the following. Taking $\tilde{a}=0.01$ and $\nu=0.3$, it is found that when $\sigma=1$, $G_{el}(\tilde{q},\varphi=0) > G_{el}(\tilde{q},\varphi=\pi)$ and $G_{el}(\tilde{q},\varphi=0) > 0$ such that in-phase fluctuations may grow faster than the antiphase ones in the case of isotropic epitaxy. The range $[\tilde{q}_{el}^{min},\tilde{q}_{el}^{max}]$ of $\tilde{q}$ values for which antiphase fluctuations are dominating so that $G_{el}(\tilde{q},\varphi=\pi) - G_{el}(\tilde{q},\varphi=0) > 0$ and $G_{el}(\tilde{q},\varphi=\pi) > 0$ has been then displayed in Figs. 2(a) and 2(b) as a function of σ. It can be observed that for anisotropic epitaxial stresses such that $\sigma \in [-3.1,-1.92]$ and $\sigma \in [1.2,3.1]$, the pinched shape may be, thus, selected. To determine now, in which conditions on the full stress tensor $(\sigma_{xx}^0,\sigma_{yy}^0)$, the development of perturbations is favorable in the linear regime, the growth rate G has been plotted in Figs. 3 as a function of $\tilde{q}$ for different values of σ and β coefficients. For the discussion, the following two levels of stress are selected, $\beta=0.19$ or $|\sigma_{xx}^0| = \sqrt{0.19\pi E\gamma/[4(1+\nu)]}/h$ and $\beta=1.6$ or $|\sigma_{xx}^0| = \sqrt{1.6\pi E\gamma/[4(1+\nu)]}/h$ which correspond to low and high σ_{xx}^0 stress, respectively. In the case where the epitaxy is isotropic ($\sigma=1$), the straight stripe remains stable for the lower stress value $\beta=0.19$ since in Fig. 3(a), $G<0$ whatever $\tilde{q}$ for $\varphi=0$ or π. In Fig. 3(b), it is found that for higher stress ($\beta=1.6$) and $\tilde{q} \in [\tilde{q}_c^{min},\tilde{q}_c^{max}]$, the growth rate of the in-phase fluctuations is positive and greater than the growth rate of the antiphase fluctuations so that the serpentine shape is kinetically selected. For the anisotropic case ($\sigma=2$), two results have to be underlined: (i) the stress anisotropy leads to stripe instability even for lower stress ($\beta=0.19$) and (ii) the antiphase growth rate is positive and greater than the in-phase one for $\tilde{q} \in [\tilde{q}_c^{min},\tilde{q}_c^{max}]$ such that now it is the pinched shape

which is kinetically selected in this particular range of $\tilde{q}$ values [see from Fig. 3(a)]. It can also be emphasized that in Eqs. (1) and (2), surface stress has been neglected so that the force amplitude does not depend on the width of the stripe. For narrow stripes, surface stress presents some size dependence so that, as shown in [35], there should be $f_x^{(k)}(\rho) = -h\sigma_{xx}^0(1+A/l)\delta(\rho-\rho_k)n_x^{(k)}$ and $f_y^{(k)}(\rho) = -h\sigma_{yy}^0\delta(\rho-\rho_k)n_y^{(k)}$, where A is a constant that can be determined from atomistic calculation of surface stress tensor. In other words, surface stress effects will enhance the anisotropic effect that has been described in this Brief Report. Obviously the smaller the local width, the greater this enhancement. It is thus clear that surface stress should be taken into account in a complete numerical study but can be neglected in the linear approach where only the onset of the stripe instability is studied.

In this Brief Report, a linear stability analysis has been performed to investigate the onset of the stress-induced destabilization of a stripe. It is found that anisotropic heteroepitaxial stresses between a stripe and its substrate strongly modify the morphological evolution of the stripe in its linear regime of evolution. Although a serpentine-like stripe develops when the epitaxial stresses is isotropic, a pinched shape preferentially emerges in the anisotropic case for selected components of stress. Finally, it is believed that the numerical study of the nonlinear regime of the stripe evolution would give relevant information on the selection of the final morphology of the stripe on a large time scale and would allow to produce a "phase diagram" characterizing the stripe morphology in the $(\sigma_{xx}^0, \sigma_{yy}^0)$ plane whose the determination is beyond the scope of the present work. In the configuration where a pinched shape would be proved to emerge from the nonlinear regime, it would also deserve to investigate the possibility of final splitting of the stripe and of the formation of a distribution of dots.

[1] W. K. Burton, N. Cabrera, and F. C. Frank, Philos. Trans. R. Soc. Lond. A **243**, 299 (1951).
[2] G. S. Bales and A. Zangwill, Phys. Rev. B **41**, 5500 (1990).
[3] C. Misbah, O. Pierre-Louis, and Y. Saito, Rev. Mod. Phys. (to be published).
[4] D.-J. Liu, J. D. Weeks, and D. Kandel, Phys. Rev. Lett. **81**, 2743 (1998).
[5] A. V. Latyshev, A. L. Aseev, A. B. Krasilnikov, and S. I. Stenin, Surf. Sci. **213**, 157 (1989).
[6] M. Dufay, J.-M. Debierre, and T. Frisch, Phys. Rev. B **75**, 045413 (2007).
[7] S. Stoyanov, Jpn. J. Appl. Phys., Part 1 **30**, 1 (1991).
[8] J. Chang, O. Pierre-Louis, and C. Misbah, Phys. Rev. Lett. **96**, 195901 (2006).
[9] O. Pierre-Louis, Phys. Rev. Lett. **96**, 135901 (2006).
[10] F. Leroy, P. Müller, J. J. Métois, and O. Pierre-Louis, Phys. Rev. B **76**, 045402 (2007).
[11] F. Leroy, D. Karashanova, M. Dufay, J. M. Debierre, T. Frisch, J. J. Métois, and P. Müller, Surf. Sci. **603**, 507 (2009).
[12] P. Müller and A. Saul, Surf. Sci. Rep. **54**, 157 (2004).
[13] B. Houchmandzadeh and C. Misbah, J. Phys. I **5**, 685 (1995).
[14] S. Paulin, F. Gillet, O. Pierre-Louis, and C. Misbah, Phys. Rev. Lett. **86**, 5538 (2001).
[15] D.-H. Yeon, P.-R. Cha, J. S. Lowengrub, A. Voigt, and K. Thornton, Phys. Rev. E **76**, 011601 (2007).
[16] A. Brodde, K. Dreps, J. Binder, Ch. Lunau, and H. Neddermeyer, Phys. Rev. B **47**, 6609 (1993).
[17] J. Shen, R. Skomski, M. Klaua, H. Jenniches, S. S. Manoharan, and J. Kirschner, Phys. Rev. B **56**, 2340 (1997).
[18] J. Shen, M. Klaua, P. Ohresser, H. Jenniches, J. Barthel, Ch. V. Mohan, and J. Kirschner, Phys. Rev. B **56**, 11134 (1997).
[19] N. N. Negulyaev, V. S. Stepanyuk, W. Hergert, P. Bruno, and J. Kirschner, Phys. Rev. B **77**, 085430 (2008).
[20] P. Gambardella, M. Blanc, L. Burgi, K. Kuhnke, and K. Kern, Surf. Sci. **449**, 93 (2000).
[21] P. Gambardella, A. Dallmeyer, K. Maiti, M. C. Malagoli, and W. Eberhardt, Nature (London) **416**, 301 (2002).
[22] K. Kern, H. Niehus, A. Schatz, P. Zeppenfeld, J. Goerge, and G. Comsa, Phys. Rev. Lett. **67**, 855 (1991).
[23] N. Silvis-Cividjian, C. W. Hagen, P. Kruit, M. A. J. d. Stam, and H. B. Groen, Appl. Phys. Lett. **82**, 3514 (2003).
[24] V. I. Marchenko and A. Y. Parshin, Sov. Phys. JETP **54**, 129 (1980).
[25] J. Tersoff and R. M. Tromp, Phys. Rev. Lett. **70**, 2782 (1993).
[26] J. Tersoff and F. K. LeGoues, Phys. Rev. Lett. **72**, 3570 (1994).
[27] R. Kern and P. Müller, Surf. Sci. **392**, 103 (1997).
[28] O. L. Alerhand, D. Vanderbilt, R. D. Meade, and J. D. Joannopoulos, Phys. Rev. Lett. **61**, 1973 (1988).
[29] W. K. Simon, E. K. Akdogan, and A. Safari, J. Appl. Phys. **97**, 103530 (2005).
[30] B. Z. Rameev, A. Gupta, G. Miao, G. Xiao, F. Yildiz, L. R. Tagirov, and B. Aktas, Tech. Phys. Lett. **31**, 802 (2005).
[31] S. Baudot, F. Andrieu, F. Rieutord, and J. Eymery, J. Appl. Phys. **105**, 114302 (2009).
[32] M. Gailhanou, A. Loubens, J. S. Micha, B. Charlet, A. A. Minkevich, R. Fortunier, and O. Thomas, Appl. Phys. Lett. **90**, 111914 (2007).
[33] L. D. Landau and E. M. Lifchitz, *Theory of Elasticity*, 3rd ed. (Pergamon, New York, 1986).
[34] N. Junqua and J. Grilhé, Acta Metall. **32**, 2139 (1984).
[35] P. Müller, P. Turban, L. Lapena, and S. Andrieu, Surf. Sci. **488**, 52 (2001).